Intermetallics 86 (2017) 116–120

Contents lists available at ScienceDirect

Intermetallics

journal homepage: www.elsevier.com/locate/intermet

Large exchange bias effect in the super spin glass state of $Mn_{50}Ni_{38}Al_{12}$ alloy

H. Pan [a], L. Ma [a, *], G.K. Li [a], L.Y. Jia [a], C.M. Zhen [a], D.L. Hou [a], W.H. Wang [b], E.K. Liu [b], J.L. Chen [b], G.H. Wu [b]

[a] Department of Physics, Hebei Advanced Thin Films Laboratory, Hebei Normal University, Shijiazhuang 050024, China
[b] Beijing National Laboratory for Condensed Matter Physics, Institute of Physics, Chinese Academy of Sciences, Beijing 100190, China

ARTICLE INFO

Article history:
Received 3 December 2016
Received in revised form
19 January 2017
Accepted 4 March 2017

Keywords:
Exchange bias
Super spin glass
Heusler alloys

ABSTRACT

A large exchange bias field (H_{EB}) of 5.3 kOe which so far, is the largest value found in MnNi-based alloys, was observed in $Mn_{50}Ni_{38}Al_{12}$ ribbon. DC and AC magnetic measurements show super spin glass (SSG) behavior below 130 K and superparamagnetic behavior above this temperature. Different from other systems, the pinning and pinned phases are both SSG. Due to the high content of Mn and low content of Al there exists considerable disorder in $Mn_{50}Ni_{38}Al_{12}$ which is responsible for the large H_{EB}.

1. Introduction

In recent years, exchange bias (EB) effect in the multifunctional Heusler alloys have attracted significant interests owing to its potential application in giant magnetoresistance, ultrahigh-density magnetic recording and spin valve devices [1,2]. For Heusler alloys, EB was first observed in $Ni_{50}Mn_{36}Sn_{14}$ and $Ni_{50}Mn_{25+x}Sb_{25-x}$ alloys, but the exchange bias field (H_{EB}) was just ~250 Oe [3,4]. The small H_{EB} restricts the application of these alloys. By doping Co into these systems, the H_{EB} was improved to several hundred Oe [5,6]. Recently, by changing the composition a large H_{EB} has been also observed in $Mn_{50}Ni_{40}Sn_{10}$ [7] ($H_{EB} = 1170$ Oe) and $Mn_{50}Ni_{42}Sn_8$ [8] ($H_{EB} = 3520$ Oe) alloys. It is worth mentioning that a giant H_{EB} ($H_{EB} = 33$ kOe) in $Mn_{2.4}Pt_{0.6}Ga$ has been observed by Felser et al. [9]. Taking into account that Pt (or Ga) and Ni (or Al) are in the same main group, a large H_{EB} may be obtained in MnNiAl system. Here in this work, based on the above idea, a large H_{EB} of 5.3 kOe was observed in $Mn_{50}Ni_{38}Al_{12}$. Besides, it is found that the pinning and pinned phases are both super spin glass by DC and AC magnetic measurements. Due to high content of Mn and low content of Al, there are considerable antisite disorder in MnNiAl, which is responsible for the large H_{EB}.

2. Experimental details

The precursor polycrystalline ingot of $Mn_{50}Ni_{38}Al_{12}$ with nominal composition was prepared by arc melting the pure metals (>99.9%) under an argon atmosphere. Subsequently, the ingot was melted in a quartz tube in an argon atmosphere and the melt spin technique used to obtain ribbons. The copper wheel rotated with a surface velocity of 25 m/s. The ribbons are hereafter referred as Al12, indicating that the Al content is 12 at. %. The crystal structure was identified by X-ray diffraction (XRD) using Cu Kα radiation. Magnetic properties were investigated utilizing a physical property measurement system (PPMS-9, Quantum Design, Inc.).

3. Results and discussion

Fig. 1 shows XRD patterns for Al12 at room temperature. It can be seen that the sample shows a martensitic tetragonal structure ($L1_0$) with a = b = 5.48 Å and c = 6.68 Å. Based on the valence-electron site occupation rule in Heusler alloys, Al12 in the austenitic phase has an off-stoichiometric Hg_2CuTi-type structure with 4 face center cubic sublattices (denoted as A (0,0,0), B (1/4 1/4 1/4), C (1/2 1/2 1/2) and D (3/4 3/4 3/4) along the body diagonal line), as shown in the insert of Fig. 1(b). The atom occupation form should be written as $(Mn_{12}Ni_{13})A\ (Mn_{25})B(Ni_{25})C(Al_{12}Mn_{13})D$ for the ordered case. The additional Ni13 atoms take up the MnA site and

* Corresponding author.
E-mail addresses: majimei@126.com, houdenglu@mail.hebtu.edu.cn (L. Ma).

http://dx.doi.org/10.1016/j.intermet.2017.03.003
0966-9795/

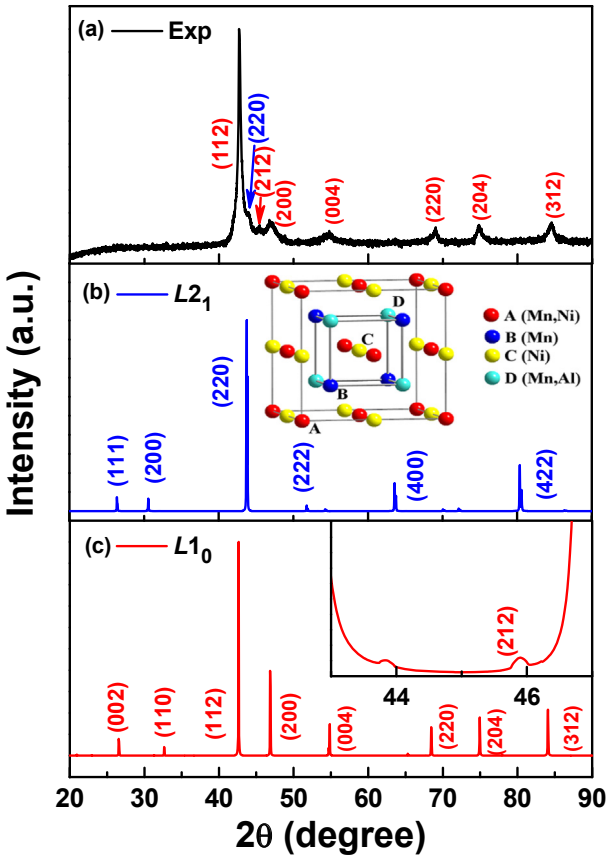

Fig. 1. (a) Experimental XRD patterns of $Mn_{50}Ni_{38}Al_{12}$ ribbon at room temperature. (b) Simulated XRD patterns of the ordered $Mn_{50}Ni_{38}Al_{12}$ with the cubic $L2_1$ structure, the insert shows the crystal structure of the $Mn_{50}Ni_{38}Al_{12}$ in the austenitic state and the atoms occupation. (c) Simulated XRD patterns of the ordered $Mn_{50}Ni_{38}Al_{12}$ with the tetragonal $L1_0$ structure, the insert shows the magnification between the (112) and (200) peaks.

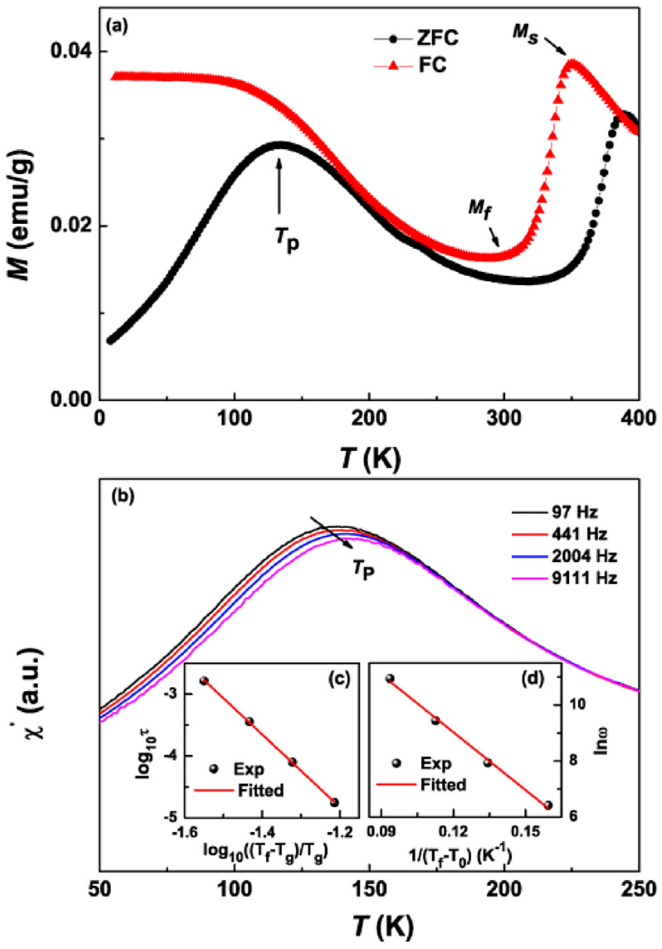

Fig. 2. (a) Thermal magnetization curves for $Mn_{50}Ni_{38}Al_{12}$ ribbon after zero field cooling and 100 Oe field cooling from 400 K to 5 K. (b) Temperature dependence of the real part of the ac susceptibility (χ′) measured at different frequencies. The arrows indicate the direction of increasing frequencies. Inserts (c) and (d) show the fitting results according to power law and the Vogel-Fulcher law, respectively.

drive commensurate Mn13 atoms to the D site. For this case, the simulated XRD patterns is obtained as shown in Fig. 1(b). Considering that the martensitic transition is a diffusionless transformation, the relative position between the atoms remains unchanged after the martensitic transition. Based on the above analysis, the simulated XRD patterns of the ordered Al12 in the martensitic state is obtained as shown in Fig. 1(c). It should be noted that the simulated XRD patterns of the ordered Al12 have two superlattice reflection peaks (002) and (110) which are absent in the experimental patterns indicating that there exists antisite disorder in Al12 ribbon. In addition, it is found that there are two additional minor peaks between (112) and (200) peaks in our experimental patterns. The first minor peak at 43.8° may correspond to the (220) peak of the cubic $L2_1$ structure, as a result of the martensitic transformation of Al12 near room temperature (~320 K). The second minor peak at 45.4° may correspond to the (212) peak of the tetragonal $L1_0$ structure as shown in the insert of Fig. 1(c), due to the preferential orientation of the ribbon sample.

Fig. 2(a) shows the zero field cooling (ZFC) and field cooling (FC) magnetization curves of Al12 in a magnetic field of 100 Oe. It can be seen that with decreasing temperature the magnetization suddenly decreases at around 350 K, which corresponds to the martensitic transformation. Here we use T_{Ms} ($T_{Ms} = 350$ K) and T_{Mf} ($T_{Mf} = 300$ K) to denote the start and finish temperatures of the martensitic transformation, respectively. Thus at room temperature we observe the martensitic structure ($L1_0$) by XRD measurement. With a further decrease in the temperature an irreversibility is observed between the ZFC and FC curves that becomes more apparent with decreasing temperature, indicating the presence of magnetically inhomogeneous phases. It is worth noting that in the ZFC curve there have a peak at $T_p = 130$ K which is usually considered to indicate the critical temperature of spin glass (SG), super spin glass (SSG) or superparamagnetic state (SPM) [10,11].

To confirm the existence of SG, SSG or SPM, we performed AC susceptibility measurements. Fig. 2(b) shows the temperature dependence of the real part of the AC susceptibility (χ′) at different frequencies (f) values. It can be seen that each curve has a distinct peak. This peak shifts toward higher temperature and its magnitude decreases with increasing frequency. In general, one can distinguish between SG-like behavior and SPM using the value of P [13]: $P = \Delta T_P/(T_P \Delta \log_{10} f)$. For SPM the interaction between the particles can nearly be neglected, and the value of P is ~0.1 [12] whereas it is ~0.01 for a SSG [13] and ~0.001 for a SG [14] system. The value of P for Al12 is 0.0168 close to the reported value of 0.016 for $Ni_2Mn_{1.4}Ga_{0.6}$ [15] indicating the SSG nature of low temperature magnetism. The SSG nature has also been further confirmed by fitting the $\chi'(T)$ data with the power law [13]: $\tau = 1/2\pi f = \tau^*(T_P/T_g - 1)^{-zv}$ and the Vogel-Fulcher law [12]: $\omega = \omega_0 \exp[-E_a/k_B(T_f - T_0)]$. In the first equation τ^* is the relaxation time of individual particle moment, T_g is the finite static